Journal of Human Evolution 63 (2012) 536–551

Contents lists available at SciVerse ScienceDirect

Journal of Human Evolution

journal homepage: www.elsevier.com/locate/jhevol

A comparative study of the trabecular bony architecture of the talus in humans, non-human primates, and *Australopithecus*

Jeremy M. DeSilva [a,*], Maureen J. Devlin [b]

[a] Department of Anthropology, Boston University, 232 Bay State Road, Boston, MA 02215, USA
[b] Center for Advanced Orthopaedic Studies, Beth Israel Deaconess Medical Center, Harvard Medical School, Boston, MA 02215, USA

ARTICLE INFO

Article history:
Received 5 April 2012
Accepted 26 June 2012
Available online 26 July 2012

Keywords:
Ankle
Trabecular bone
Wolff's Law
Hominin
Micro-computed tomography

ABSTRACT

This study tested the hypothesis that talar trabecular microarchitecture reflects the loading patterns in the primate ankle joint, to determine whether talar trabecular morphology might be useful for inferring locomotor behavior in fossil hominins. Trabecular microarchitecture was quantified in the anteromedial, anterolateral, posteromedial, and posterolateral quadrants of the talar body in humans and non-human primates using micro-computed tomography. Trabecular bone parameters, including bone volume fraction, trabecular number and thickness, and degree of anisotropy differed between primates, but not in a manner entirely consistent with hypotheses derived from locomotor kinematics. Humans have highly organized trabecular struts across the entirety of the talus, consistent with the compressive loads incurred during bipedal walking. Chimpanzees possess a high bone volume fraction, consisting of plate-like trabecular struts. Orangutan tali are filled with a high number of thin, connected trabeculae, particularly in the anterior portion of the talus. Gorillas and baboons have strikingly similar internal architecture of the talus. Intraspecific analyses revealed no regional differences in trabecular architecture unique to bipedal humans. Of the 22 statistically significant regional differences in the human talus, all can also be found in other primates. Trabecular thickness, number, spacing, and connectivity density had the same regional relationship in the talus of humans, chimpanzees, gorillas, and baboons, suggesting a deeply conserved architecture in the primate talus. *Australopithecus* tali are human-like in most respects, differing most notably in having more oriented struts in the posteromedial quadrant of the body compared with the posterolateral quadrant. Though this result could mean that australopiths loaded their ankles in a unique manner during bipedal gait, the regional variation in degree of anisotropy was similar in humans, chimpanzees, and gorillas. These results collectively suggest that the micro-architecture of the talus does not simply reflect the loading environment, limiting its utility in reconstructing locomotion in fossil primates.

Introduction

The external morphology of the primate talus has received considerable attention, including studies of comparative and functional morphology (Le Gros Clark and Leakey, 1951; Preuschoft, 1970; Lisowski et al., 1974; Fleagle, 1977; Lewis, 1980; Harrison, 1982, 1989; Conroy and Rose, 1983; Langdon, 1986; Gebo and Simons, 1987; Fleagle and Meldrum, 1988; Strasser, 1988; Gebo, 1993; Seiffert and Simons, 2001; DeSilva, 2008; Kanamoto et al., 2010; Marivaux et al., 2010). These numerous studies have been used to identify skeletal correlates of leaping, arboreal quadrupedalism, terrestrial quadrupedalism, and vertical climbing in the primate talus. Similarly, many studies have attempted to identify bipedal signals in the early hominid talus (Wood, 1974; Stern and Susman, 1983; Latimer et al., 1987; Harcourt-Smith, 2002; Gebo and Schwartz, 2006; DeSilva, 2009). As with other assessments of early hominid locomotion, these studies have yielded inconsistent conclusions, with some finding evidence for modern human-like bipedal locomotion in early hominin genera like *Australopithecus* (e.g., Latimer et al., 1987), and others suggesting that australopiths not only walked in a kinematically different manner than modern humans, but that they also spent a considerable amount of time in the trees (e.g., Stern and Susman, 1983). Perhaps one reason for these different interpretations is the remarkable variation found in the modern human talus (Lovejoy, 1978). These divergent interpretations of the hominin fossil record could be resolved if the trabecular bone of the talus

* Corresponding author.
E-mail address: jdesilva@bu.edu (J.M. DeSilva).

0047-2484/$ – see front matter © 2012 Elsevier Ltd. All rights reserved.
http://dx.doi.org/10.1016/j.jhevol.2012.06.006

produced a more sensitive signal of loading environment that can be used to reconstruct postural and locomotor behavior.

However, few published studies have attempted to characterize the internal trabecular architecture of the talus. Even in humans, the trabecular pattern of the talus has been poorly studied. von Meyer (1867) was the first to remark on the pattern of trabecular bone in a human talus. More recent studies focused on the internal architecture of the ankle joint (Takechi et al., 1982), all of the tarsals (Sinha, 1985), and specifically the talus (Pal and Routal, 1998; Ebraheim et al., 1999; Schiff et al., 2007; Athavale et al., 2008). The approach in each of these studies involved manual cross-sectioning of dry tali, followed by two-dimensional qualitative assessment of trabecular architecture. Furthermore, in each case the authors assumed that the orientations of the trabecular struts and plates faithfully follow Wolff's Law, such that the internal architecture of the talus provides a reliable signature for how forces are transmitted through the bone. Though these previous studies provide a foundation for studying talar trabecular microarchitecture, they are insufficient in several ways. First, three-dimensional quantitative techniques, such as microcomputed tomography (μCT), are more informative about trabecular microarchitecture as compared to traditional qualitative, two-dimensional measurements (Fajardo et al., 2002). Second, the use of Wolff's Law to explain the internal architecture of the talus is a circular argument. The relationship between the external loading environment and internal bony anatomy is complex, and trabecular morphology does not necessarily reflect load orientation within a joint. While experimental data from sheep (Barak et al., 2011) and guinea fowl (Pontzer et al., 2006) support the hypothesis that trabecular bone is sensitive to loading orientation, data from mice are less conclusive (Carlson et al., 2008). In primates, multiple studies report evidence for functional locomotor signals in the capitate and metacarpals (e.g., Kivell et al., 2011; Lazenby et al., 2011), metatarsals (e.g., Griffin et al., 2010), ilium and proximal femur (e.g., MacLatchy and Müller, 2002; Ryan and Ketcham, 2005; Volpato et al., 2008), and tibia, talus, and calcaneus (e.g., Maga et al., 2006; Su, 2009, 2010; Su et al., 2012). However, a recent review by Shaw and Ryan (2011) suggests that trabecular bone parameters in several joints in several different primates poorly reflect the inferred loading environment. Thus, in the current study, we consider the relationship between trabecular orientation and loading orientation as a hypothesis to be tested, rather than presumed.

The talus appears to be an ideal bone for studying the relationship between internal bony architecture and the loading environment. Previous work has shown that the trabeculae in the body of the talus in humans are almost entirely vertical, presumably to deal with the compressive forces on the ankle joint during bipedal walking (Kelikian, 2011). Horizontal plates run through the neck of the talus and into the head, perhaps reflecting the transmission of loads to the midfoot, or even reflecting the tensile forces moving through an arched foot (Takechi et al., 1982). Thus, preliminary work on the talus has shown that the trabecular patterns are relatively simple and superficially appear to be consistent with the inferred loading in the human ankle joint (Pal and Routal, 1998; Schiff et al., 2007; Athavale et al., 2008). Furthermore, the talus is the only bone in the foot that is entirely devoid of muscle, tendon, or aponeurosis attachments (Kelikian, 2011), so it may be a relatively simple model for how bone adapts to a restricted set of forces, free of the tensile forces produced by tendons and aponeuroses. Although several prominent ligaments anchor to the talus, these likely have lesser impacts on loading regime compared with muscles or tendons.

Here we report an explicit test of the hypothesis that talar trabecular bone parameters correlate with loading patterns in the primate ankle joint, and use these data to interpret fossil hominin tali. The loading environment of the human ankle joint has been reasonably well studied (e.g., Calhoun et al., 1994; Driscoll et al., 1994; Michelson et al., 2001; Corazza et al., 2005; Wan et al., 2006, 2008). Further, Schiff et al. (2007) have suggested that the trabeculae in the talus are quite sensitive to changes in loading and may reorient to deal with cartilage degeneration. Based on these studies, we have generated a predictive biomechanical model for talar mechanical loading during locomotion in humans that is independent of trabecular microarchitecture. Using information derived from kinematic studies on non-human primates, we also constructed predictive models for talar mechanical loading in non-human apes, and in semiplantigrade cercopithecoid monkeys. We then tested these models using μCT-derived three-dimensional trabecular microarchitecture from tali of extant primates. These data are used to interpret trabecular microarchitecture quantified from scans of seven tali from South African hominins recovered from the Plio-Pleistocene (1.5–2.6 Ma [millions of years ago]) cave localities of Sterkfontein, Swartkrans, and Kromdraii.

Model

Trabecular parameters measured in this study included bone volume fraction (BV/TV, %), trabecular thickness (Tb. Th., μm), trabecular separation (Tb. Sp., μm), trabecular number (Tb. #, 1/mm), connectivity density (Conn. D., 1/mm3), structural model index (SMI), and degree of anisotropy (DA) (Genant and Jiang, 2006) (Table 1). It should be noted that higher BV/TV incorporates higher Tb. # and/or higher Tb. Th. SMI reflects the average shape of the trabecular struts and plates, with values ranging from 3 for rods to 0 for plates; concave trabecular plates can actually have negative SMI values (Hildebrand and Rüegsegger, 1997). Degree of anisotropy indicates the extent to which trabeculae have no predominant orientation (isotropy, or DA = 1), with values >1 indicating progressively more oriented bone.

To compare the sensitivity of trabecular bone response to mechanical loading in differentially loaded portions of the talus, our model divides the talar body into four quadrants: anteromedial, anterolateral, posterolateral, and posteromedial (see Materials and methods for more details) (Fig. 1). Other divisions, such as anterior versus posterior or medial versus lateral, are possible, but might obscure gait-related regional morphologies. For example, an anterior–posterior division would make it difficult to detect trabecular signals of inversion/eversion, while a medial–lateral division would not reveal signals of plantarflexion/dorsiflexion. Thus, to assess both anteroposterior and mediolateral patterns of trabecular morphology, here we divide the talus into four quadrants.

Homo

While walking bipedally, forces are the highest on the ankle during heel strike and just prior to toe-off, producing a double-

Table 1
Trabecular bone parameters (Parfitt et al., 1987; Bouxsein et al., 2010).

BV/TV (%)	Bone volume fraction, or bone volume per total volume
Tb. # (/mm)	Mean trabecular number per millimeter
Tb. Th. (mm)	Mean trabecular thickness
Tb. Sp. (/mm)	Mean distance between trabeculae
Conn. D. (/mm^3)	Connectivity density; higher values indicate more connected struts
SMI	Structural model index; SMI = 0 for trabecular plates and 3 for trabecular rods; negative values correspond to concave trabecular plates
DA	Degree of anisotropy; DA = 1 for isotropic bone, >1 for progressively more oriented trabecular bone

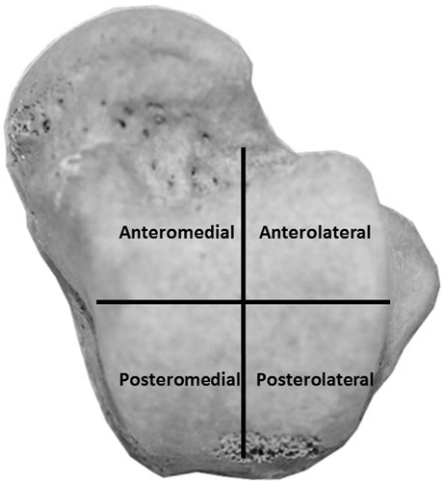

Figure 1. A human talus in dorsal view. The talus has been equally divided into four quadrants: anteromedial, anterolateral, posteromedial, and posterolateral. In this study, we divided each talus into these quadrants to test whether the underlying trabecular bone reflects the loading patterns experienced in these quadrants by different primates.

humped force curve (Kelikian, 2011). At heel-strike, the tibiotalar joint is loaded posterolaterally (Wan et al., 2006) as heel-strike generally occurs on a foot that is slightly plantarflexed and inverted relative to the long axis of the tibia (Kelikian, 2011). As stance phase progresses, the tibia internally rotates and dorsiflexes across the talar surface, such that the anterior region is loaded during much of stance phase (Wan et al., 2006). During the propulsive heel-lift and toe-off phases of walking, the foot again plantarflexes at the ankle joint, and the posterior and lateral aspect of the talus is loaded (Wan et al., 2006). Thus, our overall hypothesis is that trabecular orientation will be most anisotropic, or most oriented, in the posterolateral talar quadrant, reflecting greater trabecular alignment with the forces incurred during bipedal locomotion.

Considerable progress has been made studying the locomotor kinematics of non-human primates in both terrestrial and arboreal settings (e.g., Hirasaki et al., 1993; D'Août et al., 2002; Vereecke et al., 2003; Isler, 2005; D'Août and Vereecke, 2010; Ogihara et al., 2010), though there remain no in vivo data on the loading environment of the talus during walking and climbing in the different primates used in this study. We therefore attempted to apply what is currently known about the kinematics of the ankle in non-human apes and baboons to infer the loading environment. We suggest the following:

Papio

Cercopithecoids walk on a semiplantigrade foot (Gebo, 1992), such that the heel is raised above the substrate. During climbing bouts, cercopithecoids flex at the midfoot and experience considerably less dorsiflexion (Hirasaki et al., 1993) than what is practiced by the climbing hominoids (DeSilva, 2009). However, like the hominoids, cercopithecoids possess a foot that is in a supinated, or inverted, set. We therefore infer that the posteromedial quadrant experiences the highest loads, and the anterolateral quadrant would experience the lowest loads.

Pan and Gorilla

While gorillas are not simply scaled up chimpanzees, in the absence of detailed kinematic data on walking and climbing in the African apes, we rely on very limited kinematic data showing that chimpanzees and gorillas use their ankles in similar ways during walking and climbing. During walking, *Pan* heel-strikes simultaneously on the heel and lateral midfoot (Elftman and Manter, 1935; Gebo, 1992; Vereecke et al., 2003), and pushes-off a highly dorsiflexed ankle (D'Août et al., 2002). Furthermore, DeSilva (2009) has found that chimpanzees and gorillas dorsiflex to approximately 45° during vertical climbing bouts. Because these apes also walk and climb on a supinated foot (Wunderlich, 1999; Vereecke et al., 2003; DeSilva, 2009), we would suggest that the highest loading on the African ape ankle would be anteromedial, and the lowest posteriorly.

Pongo

DeSilva (2008) found that, as in the African apes, *Pongo* hyperdorsiflexes the foot during vertical climbing bouts, a locomotion engaged in quite often by wild orangutans (Thorpe and Crompton, 2006). Unlike the African apes, however, *Pongo* is rarely terrestrial, and therefore may be loading its ankle in a wider range of positions, including plantarflexion (Tuttle and Cortright, 1988; Thorpe and Crompton, 2006). Orangutans also have a highly supinated foot. We therefore predict that loading would be highest medially, and lowest laterally.

Hypotheses

Intraspecific trabecular architecture

H0. The null hypothesis is that there are no differences in trabecular bone parameters among the different quadrants in each primate species. This hypothesis allows an initial test of whether talar trabecular bone reflects its locomotor environment. If so, then measures of trabecular microarchitecture, including bone volume fraction, trabecular number, and/or trabecular thickness, should be greater in the quadrants that experience higher mechanical loads, and trabeculae should be more oriented in these quadrants.

H1. The primary hypothesis is that there are significant differences in trabecular bone parameters between the different quadrants, and these differences are functionally related to the loading regimes inferred for each primate species.

H2. An alternative hypothesis is that there are significant differences in trabecular bone parameters between the different quadrants, but these differences have no functional relationship to differences in loading regime in different regions of the talus.

Given the models presented above, we predict that in humans, the posterolateral talar quadrant experiences the highest loads, and would therefore have the highest BV/TV and most oriented trabecular bone. In baboons, we infer that the posteromedial quadrant experiences the highest loads, so it should have the highest BV/TV and most oriented trabecular bone, and that the anterolateral quadrant would experience the lowest loads, such that we expect lower BV/TV and less oriented bone. For gorillas and chimpanzees, we predict that the highest loading and highest BV/TV would be anteromedial, and the lowest loading and lowest BV/TV would be posterolateral. Finally, for orangutans, we predict the highest loading and highest BV/TV medially, and the lowest loading and lowest BV/TV laterally. Alternatively, if H_2 is correct, then we might observe significant intraspecific differences in trabecular morphology that do not correspond to locomotor behavior.

Interspecific trabecular architecture

H0. The null hypothesis is that there are no differences in trabecular bone parameters among the different primates.

H1. The primary hypothesis is that there are significant differences in trabecular bone parameters among the different primates, and these differences are functionally related to the different locomotor strategies practiced by these primates.

H2. An alternative hypothesis is that there are significant differences in trabecular bone parameters among the different primates, but these differences have no functional relationship to locomotor behaviors.

Our predictions from H_1 are that patterns of trabecular microarchitecture will reflect locomotor behavior across taxa. Thus, we predict the highest loads in the posterolateral quadrant will be found in bipedal humans, and will be reflected by higher posterolateral BV/TV and DA in humans versus other taxa. The highest anteromedial loads are predicted to occur in chimpanzees, gorillas, and orangutans, and the highest posteromedial loads in baboons, so we expect trabecular BV/TV and DA to correspond to these patterns. Alternatively, if H_2 is correct, then we might observe significant interspecific differences in trabecular morphology that do not correspond to locomotor behavior.

Materials and methods

Trabecular bone morphology by μCT

Assessment of bone morphology and microarchitecture was performed with microcomputed tomography. Tali of humans and non-human primates (wild shot) from the collection of the Anthropological Institute and Museum of the University of Zürich were scanned in 2008 with a Scanco μCT 80 at the same facility (Table 2). The bones were positioned using foam to produce sagittal slices of the talar body. Tali were scanned at 70 kV, with an integration time of 450 ms, and a 37 μm isotropic voxel size. Fossil tali were scanned in 2007 using medical CT scanners. Fossils (TM 1517 and SKX 42695) from the Ditsong National Museum of Natural History (formerly the Transvaal Museum) in Pretoria were scanned with a Somatom Sensation 16 at the Little Company of Mary Hospital. These scans were done with an X-ray energy of 120 keV, with a slice thickness of 1 mm. TM 1517 is regarded by most as belonging to *Paranthropus robustus*, while SKX 42695 was found in deposits that contain both *P. robustus* and *Homo erectus* and cannot be confidently assigned to either (Susman et al., 2001). Five *Australopithecus* tali listed in Table 2 were scanned with a Philips scanner at the Helen Joseph Hospital in Johannesburg, South Africa. The scans were done with the same parameters (120 keV; 1 mm thickness). These five tali were all discovered in Member 4 of the Sterkfontein cave system (Kuman and Clarke, 2000), and *Australopithecus africanus* is currently the only named hominin found in these 2.0–2.6 Ma deposits of the cave (Pickering and Kramers, 2010). Fossils are illustrated in dorsal view in Fig. 2.

Table 2
Tali scanned in this study.

Species	Male (*n*)	Female (*n*)	Unknown sex (*n*)	Total (*n*)
Papio sp.	1	4	0	5
Pongo pygmaeus	2	0	3	5
Gorilla gorilla	3	4	0	7
Pan troglodytes	3	5	0	8
Homo sapiens	2	1	4	7
Australopithecus africanus	0	0	5	5 (StW 88; StW 102; StW 347; StW 363; StW 486)
Paranthropus robustus	0	0	1	1 (TM 1517)
Homo erectus?	0	0	1	1 (SKX 42695)

Following acquisition, scans were imported into Scanco software (Scanco Medical, Brüttisellen, Switzerland) for assessment of trabecular microarchitecture. Fossil scans in DICOM format were converted to the Scanco system by reading each DICOM file into the Image Processing Language program (IPL), writing it out as an ISQ file, and finally importing it into the database (Fig. 3).

Analysis of the trabecular structure involved a segmentation of the talar body into four quadrants: anteromedial, anterolateral, posterolateral, and posteromedial (Fig. 1). This was done for two reasons. First, comparison of parameters among these quadrants would allow for a test of the sensitivity of bony response to loading in different parts of the talus in different primates. Second, the fossil and extant tali could not be compared directly because they were scanned with different CT scanners. Thus, the relative trabecular architecture in the four quadrants could be compared to test if the pattern was broadly similar between the australopithecine tali and the talus of any living primate. This issue can, and should, be revisited with the newly acquired μCT scanner at the Institute for Human Evolution (University of the Witwatersrand) in Johannesburg, South Africa.

The volumes of interest (VOIs) were contoured using the following protocol. Contouring of sagittal scans began on the first image in which the cortical bone or secondary spongiosum underlying the fibular facet was no longer visible. This slice and the slices that followed were sectioned in the coronal plane so that they contained equally divided anterior and posterior sections. Contours were manually drawn around the trabecular bone in the anterior section of the talar body for all slices. Contours were drawn such that the region of interest neared, but did not contact, the cortical shell of the talar body. Contours were copied and pasted every ten slices, and the intervening slices were contoured using the iteration tool. Each slice was then examined to be sure that the region of interest contained only trabecular bone. Slices were contoured in this manner until the cortical bone on the medial side of the talus was reached. The lateral half of these contoured slices was then evaluated at the anterolateral quadrant. The medial half of these slices was evaluated as the anteromedial quadrant. The same procedure was repeated for the posterior section of the talus.

In addition to examining the trabecular bone of the talar body, we also quantified the bone of the talar head. The head was subdivided into medial and lateral halves following the same protocol described above for the talar body.

An adaptive iterative threshold (AIT) was used to segment trabecular bone (for details see Ridler and Calvard, 1978; Trussell, 1979; Ryan and Ketcham, 2002; Maga et al., 2006; Fajardo et al., 2007). The strength of this method is that it determines the most appropriate threshold for each specimen. However, AIT may minimize real morphological differences among specimens or taxa if thresholds are widely divergent. In this case, mean AIT values determined by the software were statistically identical for humans, orangutans, and gorillas. However, both chimpanzees and baboons had significantly higher mean thresholds compared with the other taxa. We therefore re-ran the analysis with a fixed threshold set at the mean of the human and chimpanzee values. This approach did not significantly change the main results in our study. However, some relationships did lose statistical significance when evaluated with a fixed threshold. We therefore report values that were statistically significant using both the AIT and fixed threshold approach.

Trabecular parameters in the four different quadrants were compared among all of the species using nonparametric statistics. A Shapiro–Wilk test of normality was performed on the data and several parameters were not normally distributed. A Kruskal–Wallis test was used to test for significance between species, after which a Mann–Whitney *U* test was used to test for

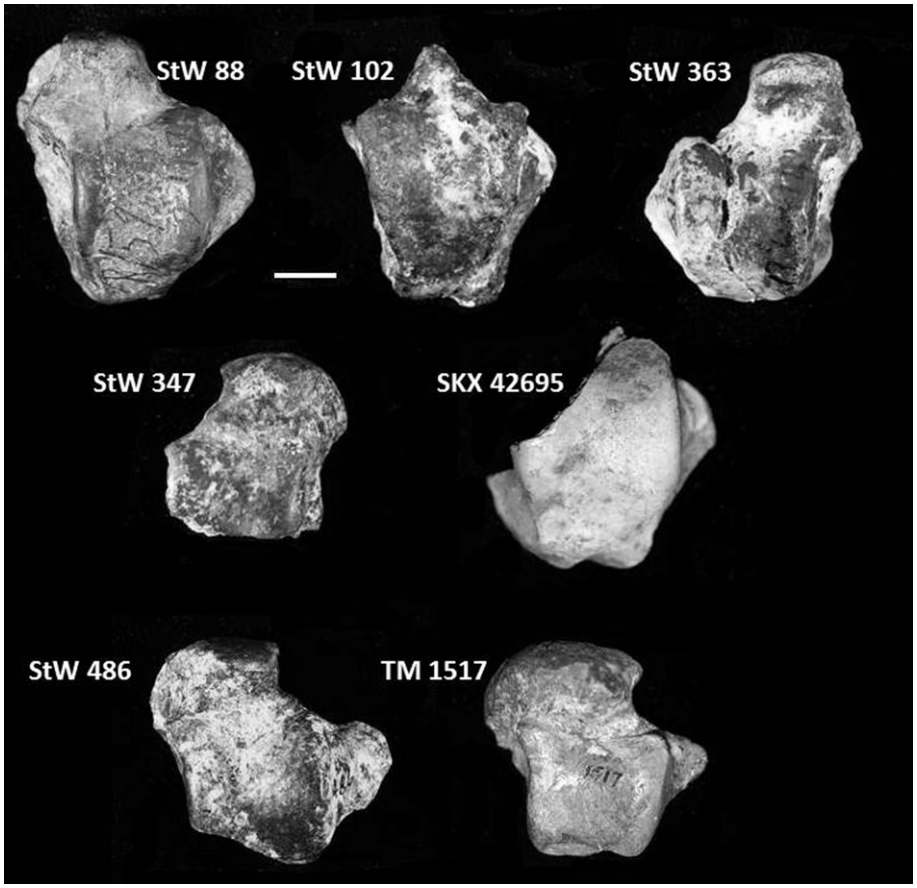

Figure 2. Fossils used in this study shown in dorsal view. StW 88, 102, 347, 363, and 486 are from Sterkfontein Member 4 and thought to be from *Australopithecus africanus*. SKX 42695 is from Swartkrans and may be from either *Paranthropus robustus* or *Homo erectus*. The TM 1517 talus from Kromdraii is most likely from a *P. robustus*. Scale bar: 1 cm.

pairwise significance. Additionally, the trabecular patterns in the four different quadrants were compared with one another within each species using a paired sample Wilcoxon test.

Results

Intraspecific results

Bone volume fraction (BV/TV, %) is consistent throughout the human talus (Fig. 4). The same is true of the orangutan talus. In the chimpanzee, posterolateral (PL) BV/TV is higher than any other quadrant. The anterolateral (AL) quadrant has a higher BV/TV than the posteromedial (PM) quadrant in the gorilla. In the baboon, anteromedial (AM) BV/TV is statistically lower than the other three quadrants, and the PL exceeds the PM.

In humans, the PL quadrant has the highest degree of anisotropy (DA), and therefore more oriented trabecular struts, but statistically higher only versus the PM quadrant (Fig. 5). The AM quadrant is slightly higher than the PM as well ($p = 0.03$). PL DA is also higher than PM in chimpanzees. In orangutans, AM DA is higher than any of the other three quadrants, while in gorillas, AL DA is higher than PM. In the baboon, PL DA is higher than AM, the opposite of what is found in orangutans.

There are no significant differences in SMI throughout the human or orangutan talus. In the chimpanzee, PL SMI is the lowest, with negative values indicating concave trabecular plates. In the gorilla, the PM quadrant is the most positive (rod-shaped) compared with the other three quadrants. In baboons, the AM quadrant has higher SMI than either posterior quadrant.

Trabecular number (Tb. #), trabecular thickness (Tb. Th.), trabecular spacing (Tb. Sp.), and connectivity density (Conn. D.) all demonstrate significant regional differences (Figs. 6–9). However, these regional differences are nearly identical in humans, chimpanzees, gorillas, and baboons. Tb. # is greatest posteriorly, followed by AL, and finally AM ($p < 0.05$ for all) (Fig. 6). Tb. Th. has the opposite pattern, with the two anterior quadrants having thicker

Figure 3. A representative human and chimpanzee talus is compared with the fossil StW 102. The specimens have been thresholded so that the trabecular bone is visualized within the shadow of the cortical shell. Quantification of the trabecular bone is explained in the text. This figure illustrates that the fossil StW 102 preserves trabecular bone, though the use of a medical scanner reduces the resolution and differing degrees of mineralization of the fossils renders some unquantifiable.

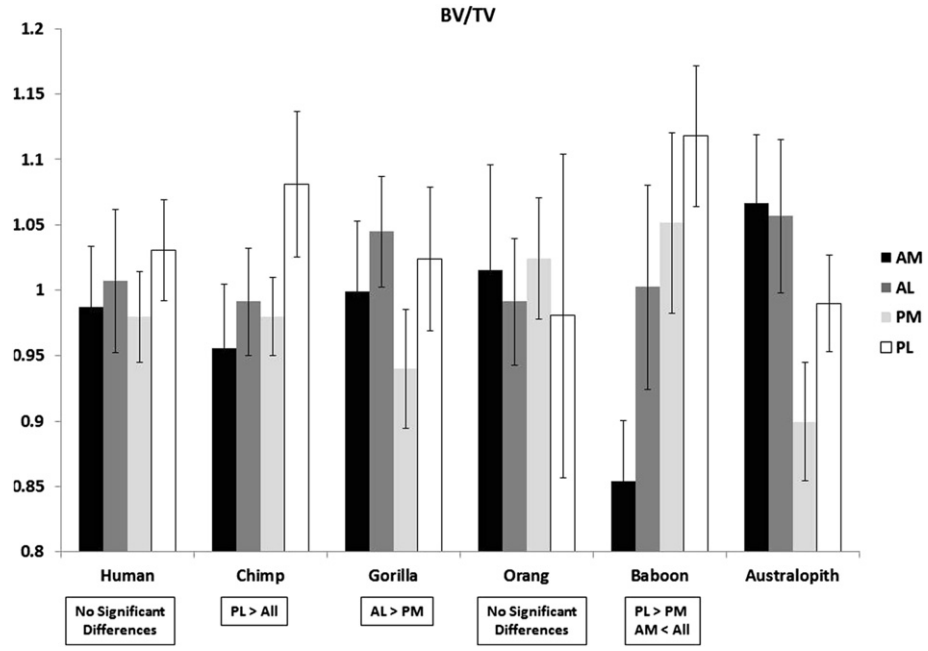

Figure 4. Relative bone volume fraction values in the four quadrants in humans, non-human primates, and *Australopithecus*. For this figure and those that follow (Figs. 4–9), the raw values have been standardized so that each quadrant would have a value of 1.0 if they were of equal value. Values above 1.0 reflect a larger relative value; values below 1.0 reflect a lower relative value. Columns represent the mean, the error bars are the standard deviation. Below each taxon is a box indicating whether any of these quadrant comparisons are statistically significant ($p < 0.05$). Note that for humans, the BV/TV values do not differ from one quadrant to another, making it most similar to orangutans. *Australopithecus* has a pattern unseen in the other primates.

struts than the PL and finally PM quadrants (with the exception of baboons and chimpanzees, in which posterior quadrants are equal) (Fig. 7). Conn. D. shows the same pattern as Tb. # (PM $\geq$ PL $>$ AL $\geq$ AM) in chimpanzees, gorillas, baboons, and humans (Fig. 8). Tb. Sp. is significantly higher in the AM versus AL quadrant, and these quadrants together have significantly higher Tb. Sp. than the posterior quadrants (with the exception of gorillas and baboons, which have equal Tb. Sp. in AL and PM quadrants) (Fig. 9). Orangutans are a notable exception, exhibiting equal Tb. # and Tb. Sp. in all four quadrants, and uniform Tb. Th. except for thicker trabeculae AL versus AM. As in other primates, the posterior quadrants have higher Conn. D. than the AL quadrant in orangutans.

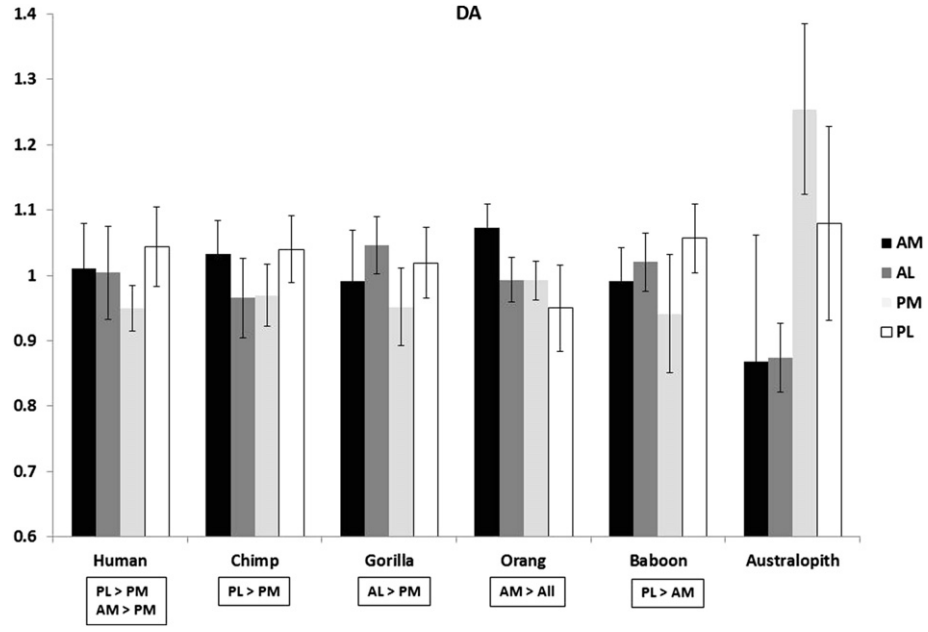

Figure 5. Relative degree of anisotropy (DA) values in the four quadrants in humans, non-human primates, and *Australopithecus*. Legend as in Figure 4. Note that humans and chimpanzees are nearly identical in having all quadrants statistically equal, except for the posterolateral being statistically higher than posteromedial. In humans, the anteromedial is statistically higher than the posteromedial, though this general trend exists in the other extant primates. *Australopithecus* has a pattern unseen in the other primates, with the posteromedial quadrant higher than the others.

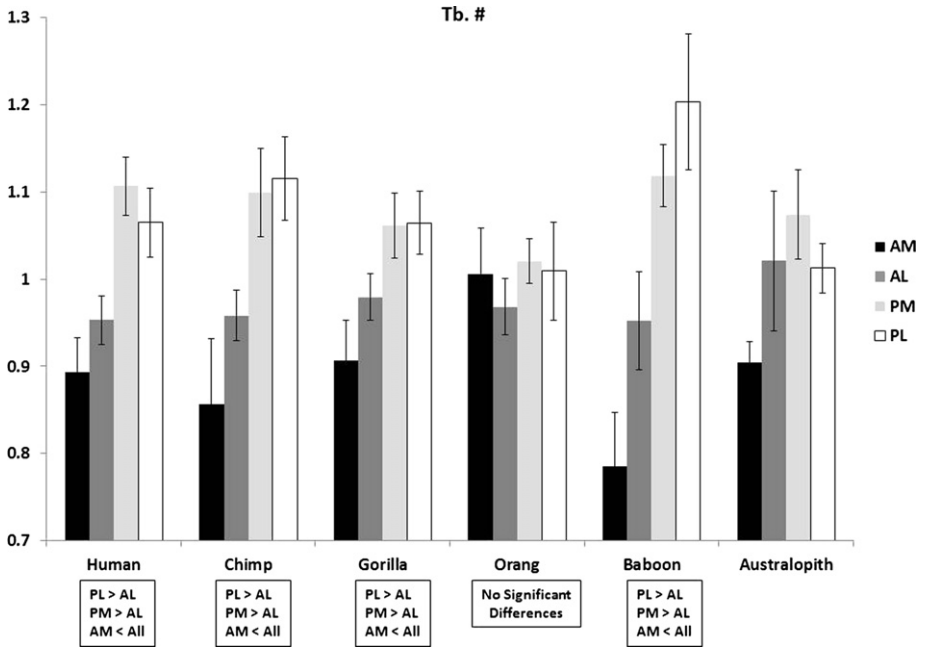

Figure 6. Trabecular number values in the four quadrants in humans, non-human primates, and *Australopithecus*. Legend as in Figure 4. Note that humans, chimpanzees, gorillas, baboons, and *Australopithecus* follow the same general pattern, with the trabecular number highest posteriorly, followed by anterolateral, and least anteromedially. Only orangutans deviate from this general pattern.

Interspecific results

Bone volume fraction (BV/TV, %) is highest in every quadrant in the chimpanzee versus other primate tali (Fig. 10). These differences are significant with humans for all quadrants, and with baboons in the AM quadrant and in the PL quadrant with orangutans. The baboon also has higher BV/TV in both posterior quadrants relative to the human ($p < 0.05$). In absolute terms, BV/TV is statistically indistinguishable in all four quadrants in humans, gorillas and orangutans, and in gorillas versus baboons.

The degree of anisotropy (DA) is uniformly high in all four quadrants of the human talus (Fig. 11). It is significantly higher than all other primates in this study in both posterior quadrants and the AL quadrant is higher than all but the orangutan. PL in the orangutan has very low DA values, significantly lower than the human, chimpanzee, and baboon. The DA of the baboon, chimpanzee, and gorilla is statistically identical in all four quadrants.

The structural model index (SMI) is quite low (indicating concave, plate-like trabeculae) in the chimpanzee talus (Fig. 12). The SMI of chimpanzees is significantly lower than all other primates in all quadrants, except for an equal SMI with the gorilla in the anterior quadrants. The gorilla also has significantly lower SMI than the human in both anterior quadrants. The baboon has a low SMI posteriorly, significantly lower than both the human and the orangutan in both quadrants. SMI is identical in all four quadrants in the human and the orangutan.

As noted above, trabecular number (Fig. 13) and thickness (Fig. 14) are quite similar across the primates sampled here. Orangutans have higher trabecular number AM versus chimpanzees, gorillas, and baboons. Baboons have a higher trabecular number PL than gorillas. Trabecular thickness mirrors these results. Orangutans have the lowest thickness AM, lower than all other primates, except baboons. AL in the orangutan has lower trabecular thickness than chimpanzees and gorillas. PL, the chimpanzee has thicker trabeculae than the human and orangutan. In absolute terms, trabecular number is identical between humans and all other primates in all four quadrants. Trabecular thickness is identical in all four quadrants in the human and gorilla, the human and baboon, chimpanzee and gorilla, chimpanzee and baboon, and finally the gorilla and baboon.

Trabecular spacing is identical in all of the primates scanned in the AL and PM quadrants (Fig. 15). In the PL quandrant, the gorilla has the highest value, significantly higher than baboons. AM, orangutans have the lowest Tb. Sp., significantly lower than all but humans. Also, baboons have a higher Tb. Sp. value than humans AM. Trabecular spacing is identical in all four quadrants of the talus in humans, chimpanzees, and gorillas. Conn. D. values are statistically higher in humans versus chimpanzees in all four quadrants (Fig. 16). Conn. D. values are also quite high in the orangutan, statistically higher than all but humans AM, and higher than the chimpanzee AL. Conn. D. values PL are significantly lower in chimpanzees compared with all but the gorilla. Humans possess identical Conn. D. values in all four talar quadrants with gorillas, orangutans, and baboons.

It is informative to see which taxa are identical for all trabecular parameters in each of the quadrants (Table 3). Chimpanzees and gorillas are statistically identical in all four quadrants for all parameters except for the higher SMI values posteriorly in the gorilla. The gorilla and the baboon are statistically identical in the AM, AL, and PM quadrants. In fact, the only characters that differ between a gorilla and baboon talus are trabecular number (higher in the baboon) and trabecular spacing (higher in the gorilla) in the PL quadrant. Posteriorly, there are no differences at all between the gorilla and the orangutan. Even primates that move in very different ways, such as the baboon and the orangutan, differ in only minor ways PM (SMI higher in the orangutan). Furthermore, posteriorly, the trabecular architecture parameters are statistically identical in humans and orangutans, with the exception of DA, which is higher in both posterior quadrants in the human. Humans and orangutans are also statistically identical for all parameters AL and differ AM only in the thicker trabecular struts in humans.

Though the focus of the study was on the talar body, we also quantified the trabecular architecture of the talar head to assess whether the orientation of the trabeculae reflected load

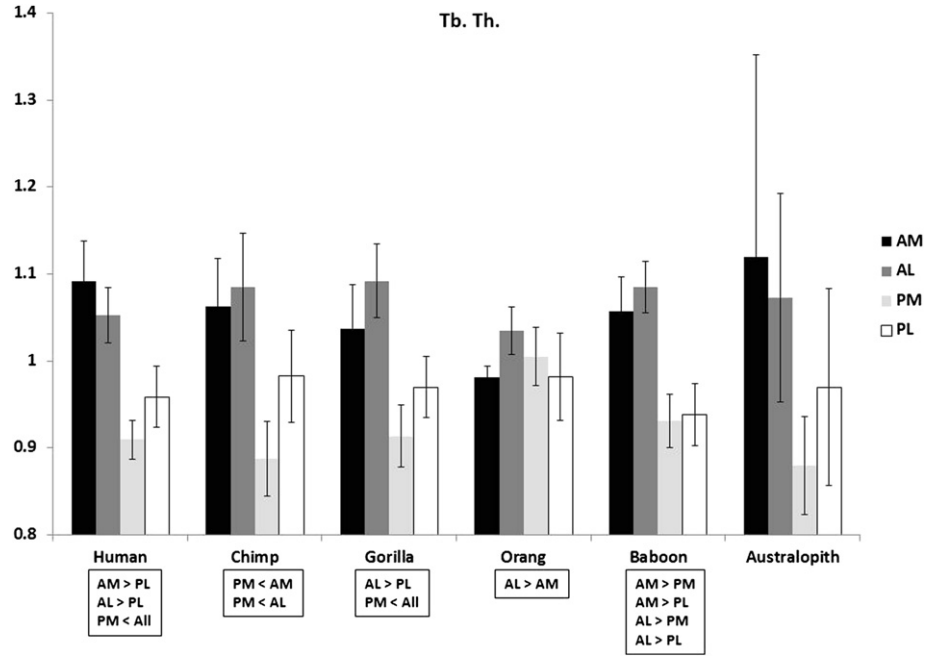

Figure 7. Trabecular thickness values in the four quadrants in humans, non-human primates, and *Australopithecus*. Legend as in Figure 4. Note that humans, chimpanzees, gorillas, baboons, and *Australopithecus* follow the same general pattern, with the trabecular thickness highest anteriorly, followed by posterolateral, and least posteromedially. Only orangutans deviate from this general pattern.

transmission through the talonavicular joint. Though the trabecular struts were more oriented in the body of the human talus compared with other primates, the head did not show the same pattern. In fact, the DA was statistically identical between humans and all other non-human primates. BV/TV and DA were higher laterally than medially in both humans and all of the non-human primates studied. The human talar head differed from the non-human primates only in possessing thicker trabeculae in the lateral portion of the talar head and more connected trabecular struts medially. All of the non-human primates possessed a higher trabecular number laterally, and more trabecular spacing medially.

Fossil scans

Two fossils are too heavily mineralized to yield any useable information: TM 1517 and StW 486. Two fossils are fragmentary, and therefore yield limited information. StW 347 preserves only the

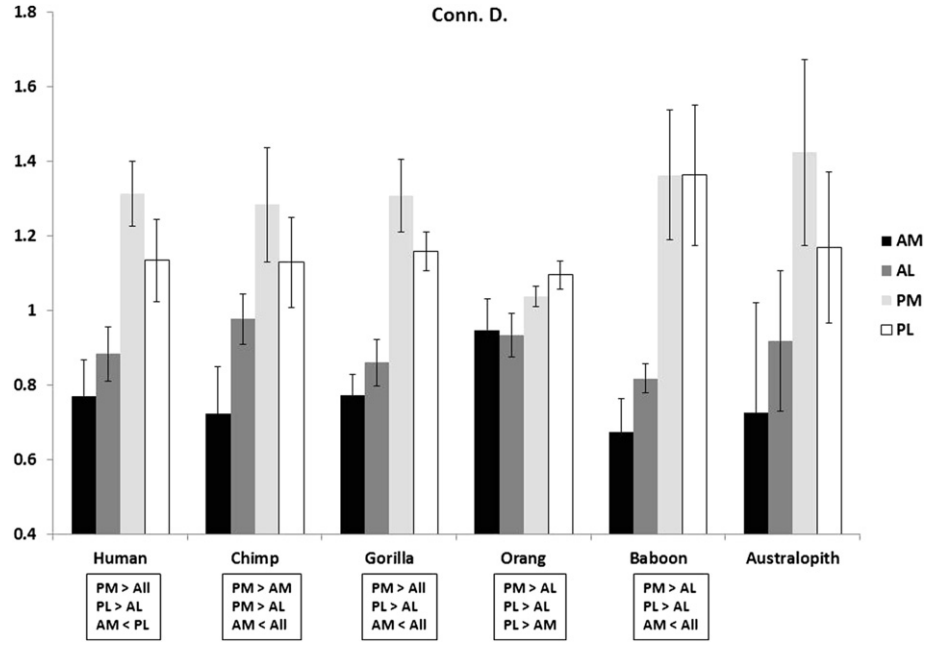

Figure 8. Connectivity density values in the four quadrants in humans, non-human primates, and *Australopithecus*. Legend as in Figure 4. Note that humans, chimpanzees, gorillas, baboons, and *Australopithecus* follow the same general pattern, with the connectivity density highest posteriorly, followed by anterolateral, and least anteromedially. Only orangutans deviate slightly from this general pattern. This pattern is almost identical to that observed in Figure 6 (trabecular number), and mirrors that found in Figs. 7 and 9 (trabecular thickness and spacing).

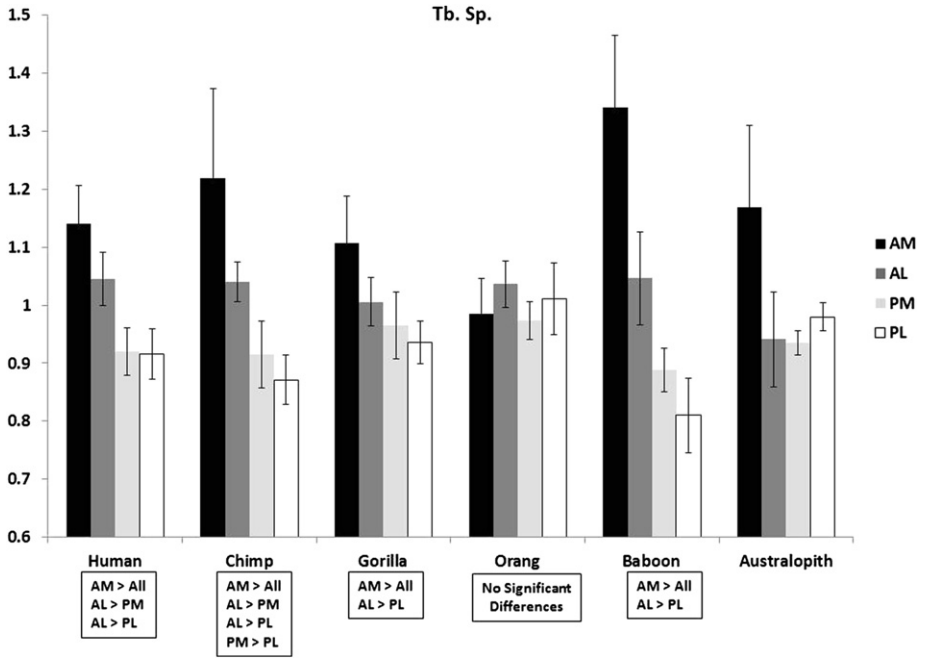

Figure 9. Trabecular spacing values in the four quadrants in humans, non-human primates, and *Australopithecus*. Legend as in Figure 4. Note that humans, chimpanzees, gorillas, baboons, and *Australopithecus* follow the same general pattern, with the trabecular spacing highest anteriorly and lowest posteriorly. Only orangutans deviate from this general pattern. This pattern is almost identical to that observed in Figure 7 (trabecular thickness), and mirrors that found in Figs. 6 and 8 (trabecular number and connectivity density).

head and the anterior portion of the talar body. SKX 42695 is broken such that the head and AM quadrant are missing. Though the trabecular bone is clearly preserved and quantifiable in these two fossils, here we focus on those bones that preserve all four quadrants of the talar body: StW 88, StW 102, and StW 363. To the extent that StW 347 could be measured, we quantified trabecular parameters and the results are consistent with those of StW 88, 102, and 363.

Because the fossil tali were scanned in a hospital scanner, and have differing levels of mineralization, direct comparisons between

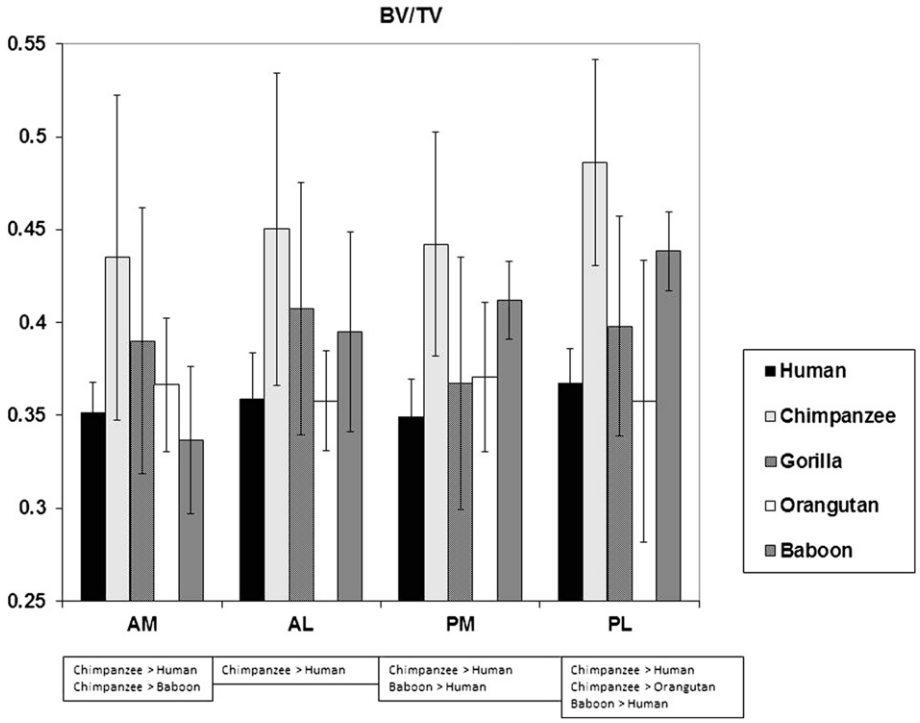

Figure 10. Interspecific comparisons between humans and non-human primates: bone volume fraction (BV/TV). The data are graphed by talar quadrant from left to right: anteromedial (AM), anterolateral (AL), posteromedial (PM) and posterolateral (PL). The columns represent means, and the error bars are the standard deviations. Below each quadrant is a box indicating whether any of these quadrant comparisons are statistically significant ($p < 0.05$). Note that the BV/TV values are highest in the chimpanzee and quite similar in the other taxa. In fact, BV/TV values in humans are statistically identical in all quadrants to the gorilla, and orangutan.

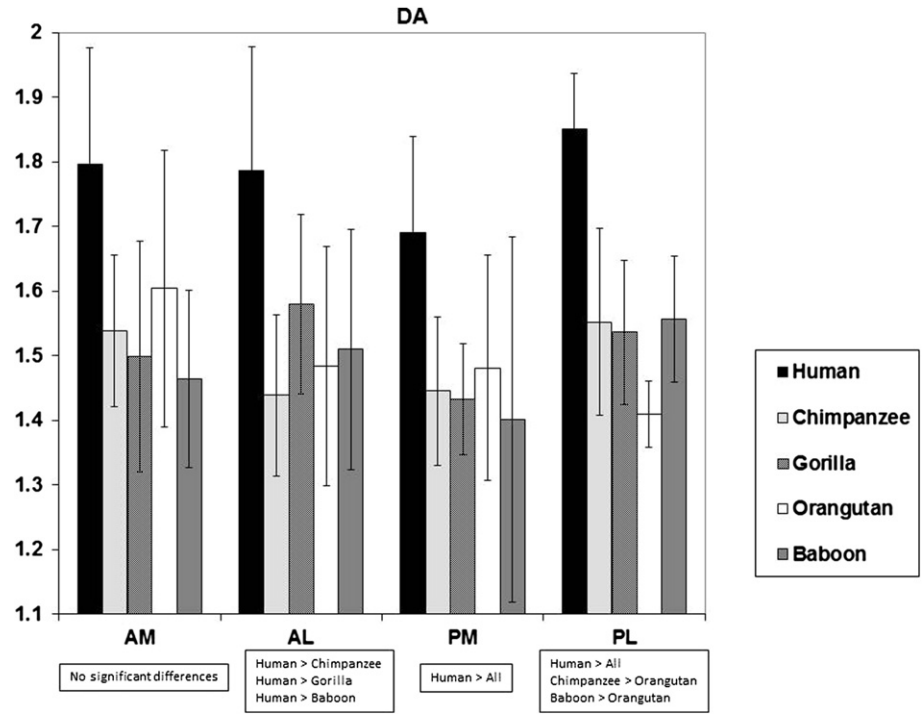

Figure 11. Interspecific comparisons between humans and non-human primates: degree of anisotropy (DA). Legend as in Figure 10. Note that the DA values are uniformly high in the human and quite similar in the other taxa.

the fossils and the extant specimens are not informative. Instead, we compared the relative values of trabecular parameters in the fossils and the extant taxa. The trabecular number, thickness, spacing, and connectivity density in the fossil tali all follow the same general pattern as that found in modern humans. This is unsurprising given what appears to be conservation in the pattern of these parameters across all of the primates in this study, with the exception of the orangutan. Thus, the AM quadrant is composed of a small number of thick trabeculae, with little connectivity and a large value of trabecular spacing. The PM quadrant is composed of

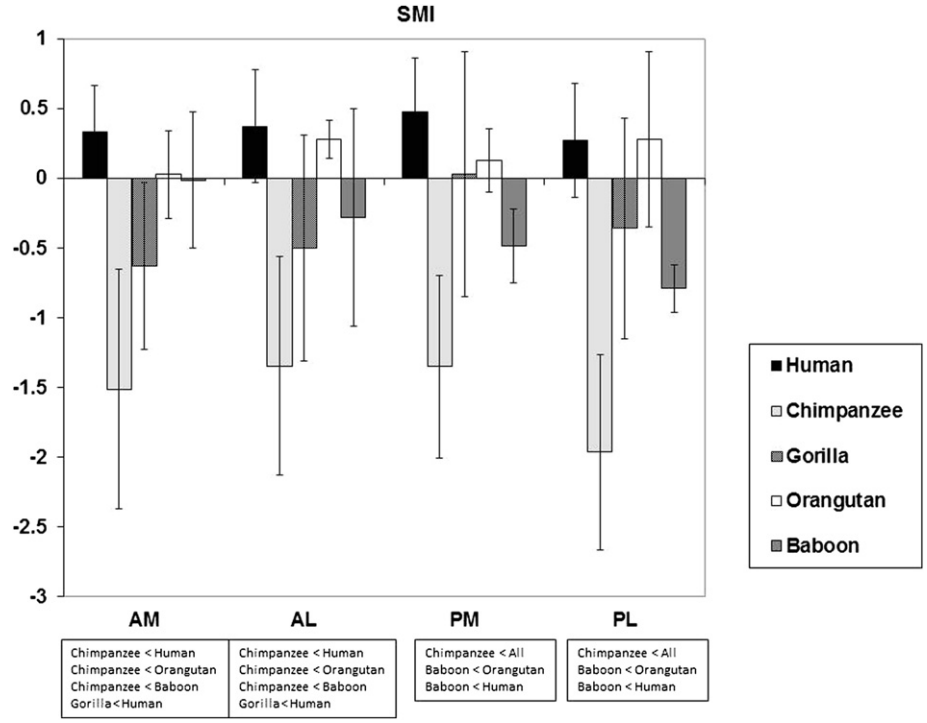

Figure 12. Interspecific comparisons between humans and non-human primates: structural model index (SMI). Legend as in Figure 10. Note that the SMI values are lowest in the chimpanzee, indicating that this ape has quite concave, plate-like trabeculae. Humans and orangutans have statistically identical SMI indices (rod-like) in the four quadrants.

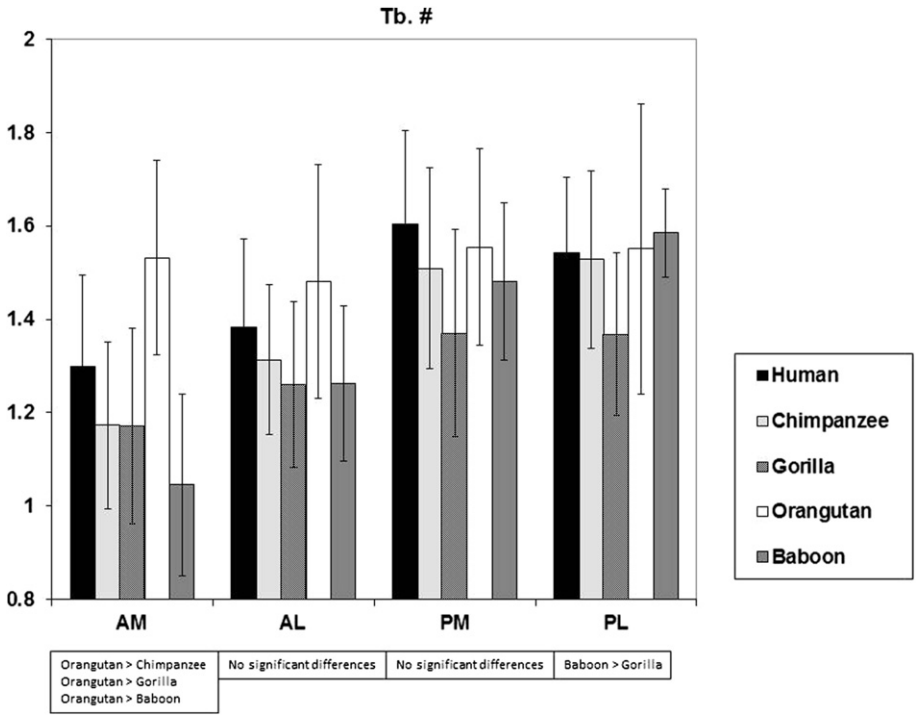

Figure 13. Interspecific comparisons between humans and non-human primates: trabecular number (Tb. #). Legend as in Figure 10. Note that trabecular number is statistically identical between humans, chimpanzees, and gorillas in all four quadrants.

a large number of thick trabeculae, all well connected, with little space between them. The other two quadrants also follow the general primate pattern. The fact that these patterns are found in the fossil tali, despite being heavily mineralized and scanned at lower resolution, suggest that the methods used to quantify fossil trabeculae in this study are sound.

In the fossil tali, the BV/TV is highest anteriorly, and lowest PM, with the PL region occupying an intermediate relative value. In this respect, the tali are most like those of gorillas. In gorillas, the AL quadrant has a statistically greater BV/TV than the PM quadrant. This relationship is unique to gorillas. In humans and chimpanzees, the BV/TV in these two quadrants is equal. In *Australopithecus*, the

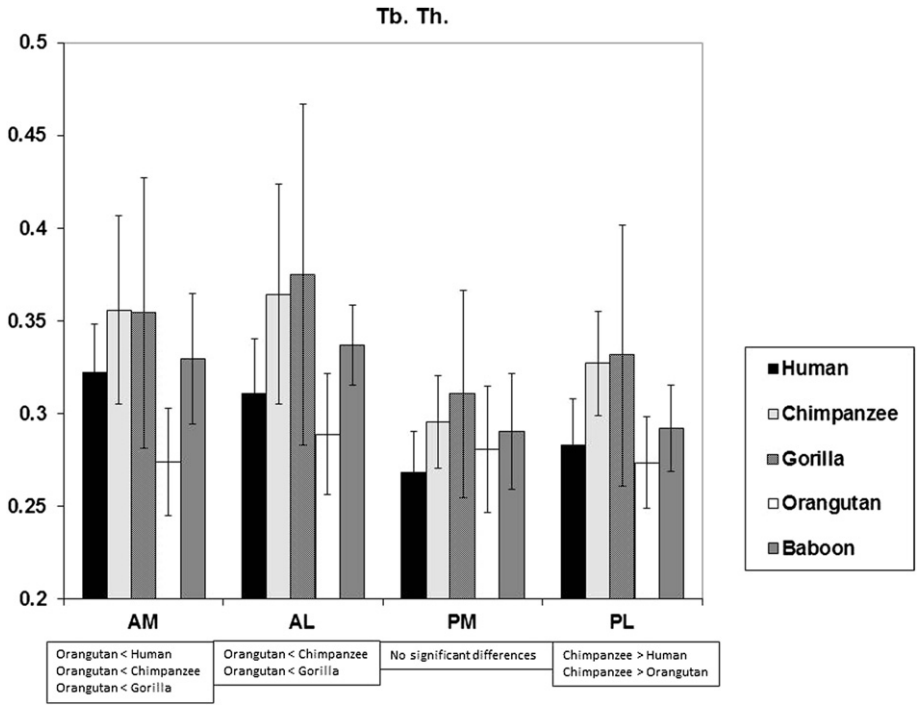

Figure 14. Interspecific comparisons between humans and non-human primates: trabecular thickness (Tb. Th.). Legend as in Figure 10. Note that trabecular thickness is statistically identical between humans and gorillas in all four quadrants. Orangutans have the thinnest trabeculae anteriorly, whereas chimpanzees and gorillas have thickest trabeculae posteriorly.

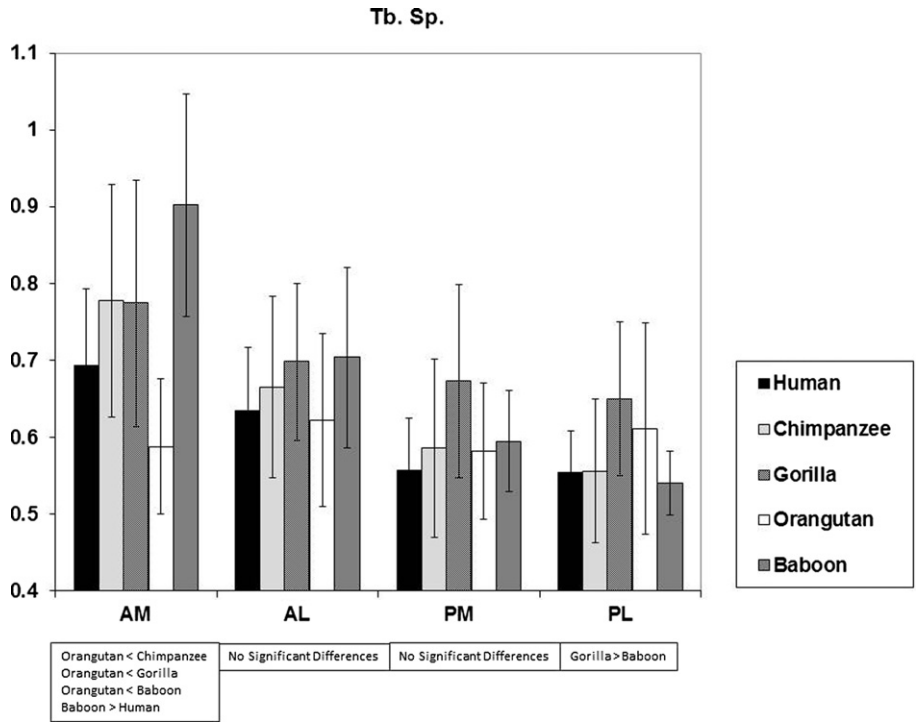

Figure 15. Interspecific comparisons between humans and non-human primates: trabecular spacing (Tb. Sp.). Legend as in Figure 10. Note that trabecular spacing is statistically identical between humans and both chimpanzees and gorillas in all four quadrants.

BV/TV value in the AL quadrant is clearly higher than the PM. However, the absolute BV/TV values of humans are identical to not only gorillas, but also to orangutans, making it difficult to make functional inferences about these fossil tali based on BV/TV values.

In all of the *Australopithecus* tali, the PM quadrant had the highest DA, which is not an ape-like feature, but instead is a unique pattern in these fossils. In humans, DA is lowest in the PM versus the other quadrants, though this relationship is also shared by

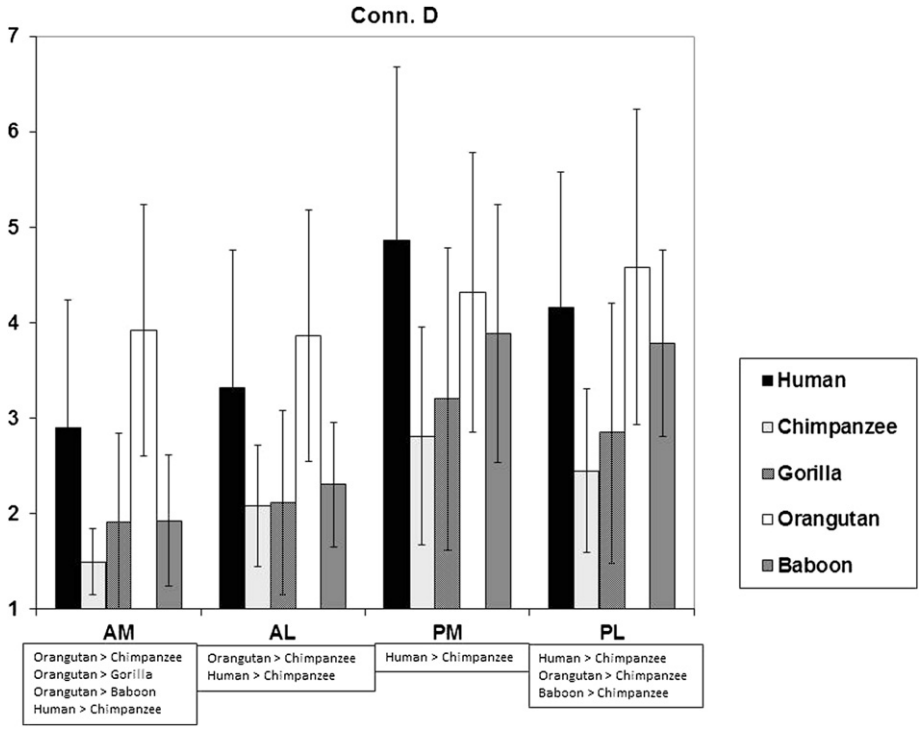

Figure 16. Interspecific comparisons between humans and non-human primates: connectivity density (Conn. D.). Legend as in Figure 10. Note that connectivity density is statistically identical between humans and orangutans for all four quadrants, and is quite high in these taxa. Conn. D. is low in the African apes.

Table 3
Interspecific similarities in quadrants of the primate talus.

Anteromedial	Anterolateral
Identical	*Identical*
Gorilla and Baboon	Human and Orangutan
Gorilla and Chimpanzee	Gorilla and Chimpanzee
	Gorilla and Baboon
	Orangutan and Baboon
One difference	*One difference*
Human and Gorilla (Human higher SMI)	Human and Baboon (Human higher DA)
Human and Orangutan (Human higher Tb. Th.)	Chimpanzee and Baboon (Baboon higher SMI)
Human and Baboon (Baboon higher Tb. Sp.)	Gorilla and Orangutan (Gorilla higher Tb. Th.)
Posteromedial	**Posterolateral**
Identical	*Identical*
Gorilla and Orangutan	Gorilla and Orangutan
Gorilla and Baboon	
One difference	*One difference*
Human and Gorilla (Human higher DA)	Human and Gorilla (Human higher DA)
Human and Orangutan (Human higher DA)	Human and Orangutan (Human higher DA)
Chimpanzee and Gorilla (Gorilla higher SMI)	Chimpanzee and Gorilla (Gorilla higher SMI)
Chimpanzee and Orangutan (Orangutan higher SMI)	
Chimpanzee and Baboon (Baboon higher SMI)	
Orangutan and Baboon (Orangutan higher SMI)	

chimpanzees, gorillas, and baboons (Table 4). Though fragmentary, three quadrants of the SKX 42695 talus could be quantified, and as is found in modern humans, the PM quadrant had the lowest DA. This similarity to modern human tali suggests that this talus may belong to *H. erectus* rather than to a robust australopithecine.

The talar heads of StW 88, StW 102, and SKX 42695 are either damaged or absent. StW 486 and TM 1517 were too highly mineralized to detect internal bone structure. The talar heads of StW 347 and StW 363 are well preserved and contain trabeculae. They are both like humans and non-human primates in possessing higher BV/TV and DA values laterally compared with medially. Like non-human primates, the trabecular spacing is higher medially, though like humans, the trabecular thickness is higher laterally.

Discussion

In this study, we used analyses of bone microarchitecture to test the hypothesis that talar trabecular bone parameters correlate with loading patterns in the primate ankle joint, both within and between taxa. We predicted that the strongest, most oriented trabecular bone in bipedal humans would be found in the posterolateral (PL) quadrant; in baboons, in the posteromedial (PM) quadrant; in gorillas and chimpanzees, in the anteromedial (AM) quadrant; and in orangutans, in the medial two quadrants. These hypotheses received mixed support at best. Rather, we found modest interspecific differences and few intraspecific differences, and these were not informative about locomotor behavior.

Overall, orangutans tend to have the thinnest, most numerous, and most connected trabeculae, especially in the anterior talar body. African apes, in contrast, have the thickest, least connected trabeculae, particularly in the PL talar quadrant. In all of the primates, except the orangutan, the trabecular number is highest posteriorly and lowest in the AM quadrant. Fossil *Australopithecus* exhibit this trend as well. The trabecular thickness is highest anteriorly, and lowest PM in all of the primates except orangutans. Again, *Australopithecus* fits this trend as well. Likewise, the connectivity density is highest posteriorly, especially PM, and lowest anteriorly, especially AM in all of the primates examined. The trabecular spacing is highest anteriorly, especially AM, and lowest posteriorly. For these measures, *Australopithecus* fits the trend of the other primates, with the exception of orangutans.

There are three results in particular that suggest to us that the trabecular bone architecture in the talus provides very little information regarding positional behavior and locomotor strategies. First, in absolute terms, gorillas and baboons have statistically identical BV/TV and DA values in all quadrants of their tali (Table 3). Baboons are semiplantigrade walkers that do very little flexed ankle vertical climbing (Rose, 1977). Lowland gorillas are

Table 4
Statistically significant features in human talus, compared with other primates.

Parameter	Relative relationship	*Australopithecus*	Chimpanzee	Gorilla	Orangutan	Baboon
DA	PL > PM		*			
	AM > PM				*	
Tb. #	PM > AL	#	*	*		*
	PM > AM	#	*	*		*
	PL > AL		*	*		*
	PL > AM	#	*	*		*
	AL > AM	#	*	*		*
Tb. Th.	AM > PM	#	*	*		*
	AM > PL	#				*
	AL > PM	#	*	*		*
	AL > PL	#		*		*
	PL > PM	#		*		
Conn. D.	PM > PL	#		*		
	PM > AL	#	*	*	*	*
	PM > AM	#	*	*		*
	PL > AL	#	*	*	*	*
	PL > AM	#	*	*	*	*
Tb. Sp.	AM > PM	#	*	*		*
	AM > PL	#	*	*		*
	AM > AL	#	*	*		*
	AL > PM	#	*			*
	AL > PL		*	*		*

= if same directional trend is observed in the australopithecine tali.
* = if the same directional trend is statistically significant in non-human primates ($p < 0.05$).

plantigrade (Gebo, 1992) and engage in frequent (Remis, 1995) flexed ankle vertical climbing (DeSilva, 2009). Finding that the two bony parameters, which explain over 80% of the variance of a bone's strength (Ulrich et al., 1999), are not just similar, but statistically identical in primates that locomote so differently implies that trabecular microarchitecture may not be responding to regional load differences. Second, humans and orangutans, quite obviously differently locomoting primates, have statistically identical trabecular bony parameters in the AL quadrant, and in the posterior quadrants of the talus differ only because of a higher degree of anisotropy in the human. In the AM quandrant, humans and orangutans differ only in humans having thicker trabeculae. Thus, of the non-human primates studied, humans have trabecular architecture most similar to that of the arboreal orangutan. However, the pattern of regional differences within the talus (Table 4) is similar to that found in African apes, not in orangutans. The bony parameters measured in this study reveal 22 statistically significant ($p < 0.05$) regional differences within the human talus. Twenty of these 22 differences exist in either the chimpanzee talus ($n = 17/22$), the gorilla talus ($n = 18/22$), or both (Table 4). Only the higher DA in the AM compared with PM quadrant and the thicker trabeculae AM versus PL is present in the human, but not in either African ape. However, neither of these relationships was expected based on kinematic data. Furthermore, African apes also show this general (though not statistically significant) trend of having more oriented and thicker bone AM relative to the posterior body of the talus. Finally, these relationships are not unique to humans, since orangutans also have higher DA in the AM quadrant relative to the PM quadrant, and baboons have significantly thicker struts AM compared with PL. Thus, there is not a single regional relationship for any of the parameters quantified in this study that is entirely singular to humans (Table 5). Given the uniqueness of human bipedal locomotion, we are surprised by these results.

This study illustrates the importance of a comparative phylogenetic approach for interpreting locomotor behavior from skeletal morphology. If we had analyzed humans alone, we might have been misled into concluding that there is strong support for Wolff's hypothesis. We predicted that humans would have the highest relative values associated with trabecular bone strength in the PL region of the talar body, and indeed, BV/TV and DA are highest in the PL region of the human talus. This pattern would seem to support our hypothesis that trabecular bone in the human talus reflects known loading orientation during bipedal walking. Further, for these measures, *Australopithecus* is quite different from modern humans, with the highest BV/TV anteriorly, in addition to PL, and the highest DA value in the PM quadrant of the bone, where it is relatively lowest in the modern human. Compared only with humans, these data would seem to support the hypothesis that the *Australopithecus* and modern human ankle joints were loaded differently. This may very well be true, however, the inability of talar trabecular bone properties to discriminate loading patterns in semiplantigrade, arboreal, knuckle-walking, and bipedal primates suggests that the trabecular architecture of the talus may not be a reliable way to infer locomotor habits in extinct primates.

Table 5
Unique regional relationships of trabecular bone architecture in the primate talus.

Genus	Parameter	Unique relative relationship
Homo	All	NONE
Pan	BV/TV	PL > AL
	SMI	AL > PL
	Tb. Sp.	PM > PL
Gorilla	BV/TV	AL > PM
	DA	AL > PM
	SMI	PM > AM
	SMI	PM > AL
Pongo	DA	AM > AL AM > PL
	Tb. Th.	AL > AM
Papio	DA	PL > AM
	SMI	AM > PM

We predicted that chimpanzees, gorillas, and orangutans would have the highest BV/TV and DA in the anterior and medial quadrants of the talus. This hypothesis is based on apes possessing a supinated foot, which, during push-off, would load the medial aspect of the ankle joint, and the fact that they both walk and climb on a highly dorsiflexed ankle, loading the anterior aspect of the joint. Contrary to our expectations, BV/TV is highest in the PL region of the talus in chimpanzees, and the pattern of BV/TV and DA in the talus in both chimpanzees and gorillas is quite similar to that seen in the human. The absolute values differ (humans have less, but more oriented, bone). However, these absolute differences appear across the entirety of the talar body, and do not appear regionally as we hypothesized. Orangutans appear to be the exception, possessing the most oriented bone (highest DA) in the AM quadrant, as hypothesized. The *Australopithecus* pattern of high BV/TV anteriorly and PL is most similar to that of the *Gorilla*, although no living taxa share its high PM DA. However, as noted above, BV/TV values are statistically identical in all quadrants of the talus in such different locomotors as the human, gorilla, and orangutan. This result alone should give serious pause to any attempts to infer locomotion in an extinct taxon based on bone volume fraction in the talus.

There are three ways to interpret these data. 1) BV/TV and DA do not vary regionally in the talus, perhaps because they are not particularly sensitive to loading in the ankle joint. 2) Our models of how African apes load their ankles during walking and climbing are incorrect or grossly oversimplified. 3) Despite the different modes of locomotion, force transmission through the ankle may happen in a very similar way in all primates. Regardless of the reason, the important result from this study is that regional differences in trabecular bony architecture do not vary in expected ways between humans and other primates, and therefore inferring locomotion from trabecular bone in fossil tali should be done with great caution. Although the absolute values differ, the patterns of BV/TV, trabecular number, thickness, connectivity density, and trabecular spacing are remarkably conserved across the primates studied here. We conclude from these data that talar trabecular microarchitecture may vary from one primate to another, but this variation is over the entire bone and may not be regionally sensitive. When the relative values are compared, there is remarkable conservation in the pattern of trabecular number, thickness, spacing and connectivity density in the different quadrants of the talus, despite quite different locomotor strategies in these different primates. Even the fossil taxon *Australopithecus* fits the general primate trend. The only exception to this rule is the orangutan, which exhibits no regional differences in trabecular number or spacing, and few regional differences in trabecular thickness or connectivity density. For these measures, it is impossible to determine whether *Australopithecus* better 'fits' the pattern seen in humans, chimpanzees, or gorillas, given the fact that the pattern of these parameters across the talus is highly conserved in the African apes and humans. We thus conclude that these characters may change globally across the entire body of the talus, but may not be regionally sensitive to different loading regimes in the primate talus, or that despite different locomotor strategies, primates (except orangutans) are loading their ankle joints in roughly the same way.

Even if the talus is not particularly sensitive to regional differences in loading, we still find that there are significant global differences in the trabecular architecture. Humans have much more oriented trabeculae across the entirety of the talus than what is

found in other primates. Additionally, there is a much lower BV/TV in the human talus than what is found in the other primates, with the possible exception of the orangutan. Chimpanzees, in contrast, appear to be unique in having a higher BV/TV, and a much lower SMI across the entirety of the talus. The negative SMI indicates the presence of concave trabecular plates in the talar body. Gorillas have this too, but not to the same degree as what is found in chimpanzees. We recommend that when fossil tali can be scanned with a μCT scanner, and not just a hospital medical scanner, that the absolute DA values may be informative in assessing whether the australopith talus has attained the human-like pattern of low BV/TV and high DA.

Conclusions

Given the methods employed in this study, we cannot make detailed inferences about the loading on the ankle joint in australopiths. All significant regional differences in the human talus can also be found in the ape or baboon talus. Furthermore, we must conclude that our original hope that the talus may be an ideal bone to study axial loading was probably incorrect. We wonder whether the absence of a growth plate may interfere with the trabecular sensitivity to loading environment observed in other studies (e.g., Pontzer et al., 2006; Barak et al., 2011). More detailed studies of the loading environment in the primate ankle, e.g., cadaver analyses, and the increasing availability of μCT-derived trabecular microarchitecture for a wider variety of skeletal elements will shed light on this question.

Acknowledgments

The authors are grateful to the University of the Witwatersrand fossil access committee for permission to study tali from Sterkfontein. We especially thank Bernhard Zipfel for access to fossils in his care and for assistance at the Helen Joseph Hospital. We thank Stephany Potze at the Ditsong National Museum of Natural History for access to fossils and transport to the Little Company of Mary Hospital. We are grateful to the technicians at both hospitals for performing these scans. Thanks to Christoph Zollikofer, Marcia Ponce de León, Naoki Morimoto, Walther Fuchs, Renaud Lebrun, and Jody Weissman at the University of Zürich for their assistance and hospitality. We thank Leeann Louis (Beth Israel Deaconess Medical Center) and Mark Blanchard (Scanco Medical) for assistance with file conversion. We thank Roberto Fajardo and Laura MacLatchy for guidance during the data acquisition stages of this project. The study was funded by the National Science Foundation (NSF BCS 0751010), and the Boston University Department of Anthropology.

References

Athavale, S.A., Joshi, S.D., Joshi, S.S., 2008. Internal architecture of the talus. Foot Ankle Int. 29, 82–86.

Barak, M.M., Lieberman, D.E., Hublin, J.J., 2011. A Wolff in sheep's clothing: trabecular bone adaptation in response to changes in joint loading orientation. Bone 49, 1141–1151.

Bouxsein, M.L., Boyd, S.K., Christiansen, B.A., Guldberg, R.E., Jepsen, K.J., Müller, R., 2010. Guidelines for assessment of bone microstructure in rodents using micro-computed tomography. J. Bone. Miner. Res. 25, 1468–1486.

Calhoun, J.H., Li, F., Ledbetter, B.R., Viegas, S.F., 1994. A comprehensive study of pressure distribution in the ankle joint with inversion and eversion. Foot Ankle Int. 15, 125–133.

Carlson, K.J., Lublinsky, S., Judex, S., 2008. Do different locomotor modes during growth modulate trabecular architecture in the murine hind limb? Integr. Comp. Biol. 48, 385–393.

Conroy, G.C., Rose, M.D., 1983. The evolution of the primate foot from the earliest primates to the Miocene hominoids. Foot Ankle 3, 342–364.

Corazza, F., Stagni, R., Castelli, V.P., Leardini, A., 2005. Articular contact at the tibiotalar joint in passive flexion. J. Biomech. 38, 1205–1212.

D'Août, K., Aerts, P., De Clercq, D., De Meester, K., Van Elsacker, L., 2002. Segment and joint angles of hind limb during bipedal and quadrupedal walking of the bonobo (*Pan paniscus*). Am. J. Phys. Anthropol. 119, 37–51.

D'Août, K., Vereecke, E., 2010. Primate Locomotion. Linking Field and Laboratory Research. Springer, New York.

DeSilva, J.D., 2008. Vertical climbing adaptations in the anthropoid ankle and midfoot: implications for locomotion in Miocene catarrhines and Plio-Pleistocene hominins. Ph.D. Dissertation, University of Michigan.

DeSilva, J.D., 2009. Functional morphology of the ankle and the likelihood of climbing in early hominins. Proc. Natl. Acad. Sci. U S A 106, 6567–6572.

Driscoll, H.L., Christensen, J.C., Tencer, A.F., 1994. Contact characteristics of the ankle joint. Part 1. The normal joint. J. Am. Podiatr. Med. Assoc. 84, 491–498.

Ebraheim, N.A., Sabry, F.F., Nadim, Y., 1999. Internal architecture of the talus: implication for talar fracture. Foot Ankle Int. 20, 794–796.

Elftman, H., Manter, J., 1935. Chimpanzee and human feet in bipedal walking. Am. J. Phys. Anthropol. 20, 69–79.

Fajardo, R.J., Müller, R., Ketcham, R.A., Colbert, M., 2007. Nonhuman anthropoid primate femoral neck trabecular architecture and its relationship to locomotor mode. J. Anat. 290, 422–436.

Fajardo, R.J., Ryan, T.M., Kappelman, J., 2002. Assessing the accuracy of high-resolution x-ray computed tomography of primate trabecular bone by comparisons with histological sections. Am. J. Phys. Anthropol. 118, 1–10.

Fleagle, J.G., 1977. Locomotor behavior and muscular anatomy of sympatric Malaysian leaf-monkeys (*Presbytis obscura* and *Presbytis melalophos*). Yearb. Phys. Anthropol. 20, 440–453.

Fleagle, J.G., Meldrum, D.J., 1988. Locomotor behavior and skeletal morphology of two sympatric pitheciine monkeys, *Pithecia pithecia* and *Chiroptes satanas*. Am. J. Primatol. 16, 227–249.

Gebo, D.L., 1992. Plantigrady and foot adaptation in African apes: implications for hominid origins. Am. J. Phys. Anthropol. 89, 29–58.

Gebo, D.L., 1993. Functional morphology of the foot in primates. In: Gebo, D.L. (Ed.), Postcranial Adaptation in Nonhuman Primates. Northern Illinois Press, DeKalb, pp. 175–196.

Gebo, D.L., Schwartz, G.T., 2006. Foot bones from Omo: implications for human evolution. Am. J. Phys. Anthropol. 129, 499–511.

Gebo, D.L., Simons, E., 1987. Morphology and locomotor adaptations of the foot in early Oligocene anthropoids. Am. J. Phys. Anthropol. 74, 83–101.

Genant, H.K., Jiang, Y., 2006. Advanced imaging assessment of bone quality. Ann. N.Y. Acad. Sci. 1068, 410–428.

Griffin, N.L., D'Août, K., Ryan, T.M., Richmond, B.G., Ketcham, R.A., Postnov, A., 2010. Comparative forefoot trabecular bone architecture in extant hominids. J. Hum. Evol. 59, 202–213.

Harcourt-Smith, W., 2002. Form and function in the hominoid tarsal skeleton. Ph.D. Dissertation, University College London.

Harrison, T., 1982. Small-bodied apes from the Miocene of East Africa. Ph.D. Dissertation, University of London.

Harrison, T., 1989. New postcranial remains of *Victoriapithecus* from the middle Miocene of Kenya. J. Hum. Evol. 18, 3–54.

Hildebrand, T., Rüegsegger, P., 1997. Quantification of bone microarchitecture with the structure model index. Comput. Method. Biomec 1, 15–23.

Hirasaki, E., Kumakura, H., Matano, S., 1993. Kinesiological characteristics of vertical climbing in *Ateles geoffroyi* and *Macaca fuscata*. Folia Primatol. 61, 148–156.

Isler, K., 2005. 3-D kinematics of vertical climbing in hominoids. Am. J. Phys. Anthropol. 126, 66–82.

Kanamoto, S., Ogihara, N., Nakatsukasa, M., 2010. Three-dimensional orientations of talar articular surfaces in humans and great apes. Primates 52, 61–68.

Kelikian, A.S., 2011. Sarrafian's Anatomy of the Foot and Ankle. Descriptive, Topographic, Functional. Lippincott Williams & Wilkins, Philadelphia.

Kivell, T.L., Skinner, M.M., Lazenby, R., Hublin, J.J., 2011. Methodological considerations for analyzing trabecular architecture: an example from the primate hand. J. Anat. 218, 209–225.

Kuman, K., Clarke, R.J., 2000. Stratigraphy, artifact industries and hominin associations for Sterkfontein, Member 5. J. Hum. Evol. 38, 827–847.

Langdon, J.H., 1986. Functional Morphology of the Miocene Hominoid Foot. Contributions to Primatology, vol. 22. Karger, New York.

Latimer, B., Ohman, J.C., Lovejoy, C.O., 1987. Talocrural joint in African hominoids: implications for *Australopithecus afarensis*. Am. J. Phys. Anthropol. 74, 155–175.

Lazenby, R.A., Skinner, M.M., Hublin, J.J., Boesch, C., 2011. Metacarpal trabecular architecture variation in the chimpanzee (*Pan troglodytes*): evidence for locomotion and tool-use? Am. J. Phys. Anthropol. 144, 215–225.

Le Gros Clark, W.E., Leakey, L.S.B., 1951. The Miocene Hominoidea of Africa. Fossil Mammals of Africa, No. 1. British Museum of Natural History, London.

Lewis, O.J., 1980. The joints of the evolving foot. Part I. The ankle joint. J. Anat. 130, 527–543.

Lisowski, F.P., Albrecht, G.H., Oxnard, C.E., 1974. The form of the talus in some higher primates: a multivariate study. Am. J. Phys. Anthropol. 41, 191–216.

Lovejoy, C.O., 1978. A biomechanical review of the locomotor diversity of early hominids. In: Jolly, C.E. (Ed.), Early Hominids of Africa. Duckworth, London, pp. 403–429.

MacLatchy, L.M., Müller, R., 2002. A comparison of the femoral head and neck trabecular architecture of *Galago* and *Perodicticus* using micro-computed tomography (μCT). J. Hum. Evol. 43, 89–105.

Maga, M., Kappelman, J., Ryan, T.M., Ketcham, R.A., 2006. Preliminary observations on the calcaneal trabecular microarchitecture of extant large-bodied hominoids. Am. J. Phys. Anthropol. 129, 410–417.

Marivaux, L., Beard, K.C., Chaimanee, Y., Dagosto, M., Gebo, D.L., Guy, F., Marandat, B., Khaing, K., Kyaw, A.A., Oo, M., Sein, C., Soe, A.N., Swe, M., Jaeger, J.J., 2010. Talar morphology, phylogenetic affinities, and locomotor adaptation of a large-bodied amphipithecid primate from the late middle Eocene of Myanmar. Am. J. Phys. Anthropol. 143, 208–222.

Michelson, J.D., Checcone, M., Kuhn, T., Varner, K., 2001. Intra-articular load distribution in the human ankle joint during motion. Foot Ankle Int. 22, 226–233.

Ogihara, N., Makishima, H., Nakatsukasa, M., 2010. Three-dimensional musculoskeletal kinematics during bipedal locomotion in the Japanese macaque, reconstructed based on an anatomical model-matching method. J. Hum. Evol. 58, 252–261.

Pal, G.P., Routal, R.V., 1998. Architecture of the cancellous bone of the human talus. Anat. Rec. 252, 185–193.

Parfitt, A.M., Drezner, M.K., Glorieux, F.H., Kanis, J.A., Malluche, H., Meunier, P.J., Ott, S.M., Recker, R.R., 1987. Bone histomorphometry: standardization of nomenclature, symbols, and units. J. Bone. Miner. Res. 2, 595–610.

Pickering, R., Kramers, J.D., 2010. Re-appraisal of the stratigraphy and determination of new U-Pb dates for the Sterkfontein hominin site, South Africa. J. Hum. Evol. 59, 70–86.

Pontzer, H., Lieberman, D.E., Momin, E., Devlin, M.J., Polk, J.D., Hallgrimsson, B., Cooper, D.M., 2006. Trabecular bone in the bird knee responds with high sensitivity to changes in load orientation. J. Exp. Biol. 209, 57–65.

Preuschoft, H., 1970. Functional anatomy of the lower extremety. In: Bourne, G.H. (Ed.). The Chimpanzee, vol. 3. Karger, Basel, pp. 221–294.

Remis, M.J., 1995. Effects of body size and social context on the arboreal activities of lowland gorillas in the Central African Republic. Am. J. Phys. Anthropol. 97, 413–433.

Ridler, S., Calvard, T.W., 1978. Picture thresholding using an iterative selection method. IEEE. Trans. Syst. Man. Cybern. 8, 630–632.

Rose, M.D., 1977. Postitional behavior of olive baboons (*Papio anubis*) and its relationship to maintenance and social activities. Primates 18, 59–116.

Ryan, T.M., Ketcham, R.A., 2002. Femoral head trabecular bone structure in two omomyid primates. J. Hum. Evol. 42, 241–263.

Ryan, T.M., Ketcham, R.A., 2005. Angular orientation of trabecular bone in the femoral head and its relationship to hip joint loads in leaping primates. J. Morphol. 265, 249–263.

Schiff, A., Li, J., Inoue, N., Masuda, K., Lidtke, R., Muehleman, C., 2007. Trabecular angle of the human talus is associated with the level of cartilage degeneration. J. Musculoskelet. Neuronal Interact 7, 224–230.

Seiffert, E.R., Simons, E.L., 2001. Astragalar morphology of late Eocene anthropoids from the Fayum Depression (Egypt) and the origin of catarrhine primates. J. Hum. Evol. 41, 577–606.

Shaw, C.N., Ryan, T.M., 2011. Does skeletal anatomy reflect adaptation to locomotor patterns? Cortical and trabecular architecture in human and nonhuman anthropoids. Am. J. Phys. Anthropol. 147, 187–200.

Sinha, D.N., 1985. Cancellous structure of tarsal bones. J. Anat. 140, 111–117.

Stern, J.T., Susman, R.L., 1983. The locomotor anatomy of *Australopithecus afarensis*. Am. J. Phys. Anthropol. 60, 279–317.

Strasser, E., 1988. Pedal evidence for the origin and diversification of cercopithecid clades. J. Hum. Evol. 17, 225–245.

Su, A., 2009. Internal bone structure in the human hind foot as an indicator of habitual compressive load during locomotion. Am. J. Phys. Anthropol. S138, 250.

Su, A., 2010. Quantitative analysis and functional significance of subchondral and cancellous bone micro-architecture in the hominid hind limb. Am. J. Phys. Anthropol. S141, 226.

Su, A., Demes, B., Carlson, K.J., 2012. The primary orientation of trabecular bone in the hominoid tibiotalar joint. Am. J. Phys. Anthropol. S147, 290.

Susman, R.L., de Ruiter, D.J., Brain, C.K., 2001. Recently identified post-cranial remains of *Paranthropus* and early *Homo* from Swartkrans Cave, South Africa. J. Hum. Evol. 41, 607–629.

Takechi, H., Ito, S., Takada, T., Nakayama, H., 1982. Trabecular architecture of the ankle joint. Surg. Radiol. Anat. 4, 227–233.

Thorpe, S.K.S., Crompton, R.H., 2006. Orangutan positional behavior and the nature of arboreal locomotion in Hominoidea. Am. J. Phys. Anthropol. 131, 384–401.

Trussell, H.J., 1979. Comments on "Picture thresholding using an iterative selection method." IEEE T. Syst. Man. Cyb 9, 311.

Tuttle, R.H., Cortright, G.W., 1988. Positional behavior, adaptive complexes, and evolution. In: Schwartz, J.H. (Ed.), Orang-Utan Biology. Oxford University Press, Oxford, pp. 311–330.

Ulrich, D., van Rietbergen, B., Laib, A., Rüegsegger, P., 1999. The ability of three-dimensional structural indices to reflect mechanical aspects of trabecular bone. Bone 25, 55–60.

Vereecke, E., D'Août, K., De Clercq, D., Van Elsacker, L., Aerts, P., 2003. Dynamic plantar pressure distribution during terrestrial locomotion in bonobos (*Pan paniscus*). Am. J. Phys. Anthropol. 120, 373–383.

Volpato, V., Viola, T.B., Nakatsukasa, M., Bondioli, L., Macchiarelli, R., 2008. Textural characteristics of the iliac-femoral trabecular pattern in a bipedally trained Japanese macaque. Primates 49, 16–25.

von Meyer, G.H., 1867. Die Architektur der Spongiosa. Arch. Anat. Physiol. Wiss. Med. 34, 615–628.

Wan, L., de Asla, R.J., Rubash, H.E., Li, G., 2006. Determination of in-vivo articular cartilage contact areas of human talocrural joint under weightbearing conditions. Osteoarthr. Cartilage 14, 1294–1301.

Wan, L., de Asla, R.J., Rubash, H.E., Li, G., 2008. In vivo cartilage contact deformation of human ankle joints under full body weight. J. Orthop. Res. 26, 1081–1089.

Wood, B.A., 1974. Evidence on the locomotor pattern of *Homo* from early Pleistocene of Kenya. Nature 251, 135–136.

Wunderlich, R., 1999. Pedal form and plantar pressure distribution in anthropoid primates. Ph.D. Dissertation, State University of New York at Stony Brook.